

# A new approach for studying aqueous phase OH kinetics: application of Teflon waveguides

Christian George,\* Davy Rousse, Emilie Perraudin† and Rafal Strekowski

Laboratoire d'Application de la Chimie à l'Environnement (UCBL-CNRS) 43 boulevard du 11 Novembre 1918, F-69622, Villeurbanne, France. E-mail: christian.george@univ-lyon1.fr; Fax: +33 (0)4 72 44 8114; Tel: +33 (0)4 72 43 1489

Received 28th January 2003, Accepted 26th February 2003  
First published as an Advance Article on the web 12th March 2003

Bimolecular rate coefficients for the reactions of the hydroxyl radical, OH, with methanol, ethanol, tetrahydrofuran, dimethylmalonate [ $\text{CH}_3\text{OC}(\text{O})\text{CH}_2\text{C}(\text{O})\text{OCH}_3$ ], dimethylsuccinate [ $\text{CH}_3\text{OC}(\text{O})\text{CH}_2\text{CH}_2\text{C}(\text{O})\text{OCH}_3$ ], dimethylcarbonate [ $\text{CH}_3\text{OC}(\text{O})\text{OCH}_3$ ] and diethylcarbonate [ $\text{CH}_3\text{CH}_2\text{OC}(\text{O})\text{OCH}_2\text{CH}_3$ ] in aqueous solutions have been measured using a novel experimental approach. The centrepiece of the new experimental technique reported in this work is a Teflon AF 2400 liquid core waveguide. The physical properties of the Teflon AF 2400 liquid core waveguide allow for the construction of a micro-flowtube reaction photolysis cell with an extremely low volume and a very long optical pathway. Such a reaction system allows for a very sensitive detection of chemical transients in the aqueous phase. The micro-flowtube experiments involved competition kinetics of the OH radical with the organic reactant of interest and an  $\text{SCN}^-$  anion, ( $k_{\text{OH}+\text{SCN}^-} = 1.29 \times 10^{10} \text{ M}^{-1} \text{ s}^{-1}$ ).<sup>1</sup> The  $(\text{SCN})_2^-$  anion was detected using UV-visible spectroscopy following a medium pressure mercury lamp photolysis ( $\lambda \geq 366 \text{ nm}$ ) of  $\text{H}_2\text{O}/\text{H}_2\text{O}_2$ /reactant/KSCN mixtures. All experiments were carried out at room temperature. Measured rate coefficients for the reaction of the OH radical with methanol, ethanol, tetrahydrofuran, dimethylmalonate, dimethylsuccinate, dimethylcarbonate and diethylcarbonate are (units are  $10^8 \text{ M}^{-1} \text{ s}^{-1}$ ):  $k_{\text{OH}+\text{methanol}} = 13 \pm 4$ ,  $k_{\text{OH}+\text{ethanol}} = 19 \pm 5$ ,  $k_{\text{OH}+\text{THF}} = 38 \pm 10$ ,  $k_{\text{OH}+\text{dimethylmalonate}} = 2.7 \pm 0.9$ ,  $k_{\text{OH}+\text{dimethylsuccinate}} = 5.3 \pm 2.9$ ,  $k_{\text{OH}+\text{dimethylcarbonate}} = 0.51 \pm 0.22$ ,  $k_{\text{OH}+\text{diethylcarbonate}} = 7.9 \pm 3.2$ . Uncertainties in the above expressions are  $\pm 2\sigma$  and represent precision only. The reported rate coefficients for the reactions of OH with ethanol, methanol and THF agree very well with the currently recommended values. To date, there is no kinetic data reported in the literature for the OH radical reaction with dimethylmalonate, dimethylsuccinate, dimethylcarbonate and diethylcarbonate. The reaction mechanism is briefly discussed as a function of bond energies.

## Introduction

Both in the gas phase and in aqueous droplets (*i.e.*, hydrometeors) the hydroxyl radical is the most important daytime oxidizing agent responsible for the atmospheric degradation of most of the volatile organic compounds (VOCs).<sup>2</sup> To date, the reaction kinetics of the OH radical toward a large number of organic species have been reported (see, for example, the readily available solution kinetic database<sup>3</sup>). Although many studies of the kinetics of the OH +  $\text{C}_1$  to  $\text{C}_2$  compounds or OH + long chain hydrocarbons (*i.e.*, of biological interest) reactions are reported in the literature, very few studies have been performed for the reactions of OH with the intermediate sized aliphatic compounds (*i.e.*,  $\text{C}_2$ – $\text{C}_{10}$ ), and especially for the reactions of OH with organics containing oxygenated poly-functional groups.

The interest in the OH reactions mentioned above, stems from the fact that the intermediate length carbon chain and oxygenated hydrocarbon compounds are expected to be increasingly used as new industrial solvents to favour water based technology. Currently,  $\text{C}_2$ – $\text{C}_{10}$  dibasic esters<sup>4–6</sup> and carbonates<sup>7,8</sup> are being considered to replace “old” additives to

obtain “new” environmentally friendly solvents. However, the atmospheric degradation of dibasic esters and carbonates will potentially result in the formation of tropospheric ozone and other secondary pollutants.<sup>5</sup> Moreover, the  $\text{C}_2$ – $\text{C}_{10}$  oxygenated organics can potentially form low vapour pressure secondary reaction species that can be either taken up by clouds or form secondary aerosols<sup>9,10</sup> (SOA). In turn, these compounds can be removed from the atmosphere *via* rain, dry or wet deposition and potentially act as a source of organic pollutants in surface waters.

To date, the atmospheric fate of  $\text{C}_2$ – $\text{C}_{10}$  dibasic esters and carbonates remains uncertain. In the atmosphere these compounds are likely to be involved in multiphase chemistry and be removed *via* the attack by OH. One large volume chamber study of the reaction of the OH radical with the dibasic ester  $\text{CH}_3\text{OC}(\text{O})\text{CH}_2\text{CH}_2\text{CH}_2\text{C}(\text{O})\text{OCH}_3$ , DBE-5, in the presence of nitric oxide suggests that organic nitrate(s), mono-methyl glutarate, [ $\text{CH}_3\text{OC}(\text{O})\text{CH}_2\text{CH}_2\text{CH}_2\text{C}(\text{O})\text{OH}$ ] and dimethyl 1,3-acetonedicarboxylate account for  $77 \pm 27\%$  of the total reaction products and reaction pathways.<sup>11</sup> In this paper, we present the results of the rate coefficient measurements for the liquid phase reactions of the OH radical with several oxygenated compounds of atmospheric interest using a novel experimental technique. This new technique takes advantage of the pioneering waveguide technology where the reaction cell is a micro-flowtube made of Teflon AF. To our knowledge, this is the first study to use the new Teflon AF liquid core

† Present address: Laboratoire de Physico-Chimie Moléculaire (Université Bordeaux I/CNRS) 351 cours de la Libération, 33405 Talence Cedex, France. Fax: +33 (0)5 56 84 66 45; Tel.: +33 (0)5 56 84 28 68; E-mail: e.perraudin@lpcm.u-bordeaux1.fr.

waveguide technology to study liquid phase chemical kinetics of atmospheric interest. Comparison of data using different experimental techniques is important because each technique is subject to different systematic errors.

Details of the experimental procedure that were employed to study the reactions of OH with methanol, ethanol, tetrahydrofuran, dimethylmalonate, dimethylsuccinate, dimethylcarbonate and diethylcarbonate in aqueous solutions are given below.

## Experimental

In order to study aqueous phase radical chemistry, a number of precautions have to be taken. First, radical species must be produced using the cleanest possible way (for example, photo-Fenton reactions with iron oxides may generate potential interferences).<sup>12</sup> Second, transient radical concentrations have to be small enough in order to avoid unwanted complications from secondary chemistry (for example recombination reactions). Such considerations have led over the years to the development and validation of well established experimental methods such as pulse radiolysis and laser flash photolysis techniques.<sup>13–21</sup> In most cases, radical species produced using the above techniques are coupled with UV-visible time resolved spectroscopy.

### Teflon AF waveguides

Often, when studying liquid phase reactions, when light passes through a reaction cell between two White cell mirrors, energy (or light) is lost on the windows. This problem may be overcome by using long-path cells without windows.

A “windowless” reaction cell can be achieved by using a liquid core waveguide (henceforth called LCW). For practical reasons (discussed in the following section), the LCW must (i) have a relatively small diameter, (ii) be flexible, (iii) be transparent to UV radiation (used to produce OH radicals) and (iv) have a refractive index lower than the one of water *i.e.*,  $n = 1.33$ . The latter condition is essential for the LCW in order to allow total internal reflection and, therefore, conduction of light.

To date, the only commercially available materials allowing for the conduction of light in water at room temperature are copolymers of tetrafluoroethylene and 2,2-bis(trifluoromethyl)-4,5-difluoro-1,3-dioxole sold by DuPont as Teflon AF.<sup>22,23</sup> Tubing made from these polymers has been shown to exhibit excellent optical properties, such as high optical clarity (at  $\lambda \leq 200$  nm more than 80% of light is transmitted through a 220  $\mu\text{m}$  thick film of the polymer described above) and very low refractive index (*i.e.*,  $n = 1.29$  for Teflon AF 2400 grades). The refractive index observed for the Teflon AF 2400 tube is lower than virtually all standard temperature and pressure liquids. In addition, the refractive index of  $n = 1.29$  for The Teflon AF 2400 tube is close to the theoretical minimum for an organic polymer as predicted by Groh and Zimmermann.<sup>24</sup> As a result, tubing made from the Teflon AF 2400 polymer and filled with water will conduct light. It has been shown that the optical attenuation for such tubing is less than 50% per meter of tubing.<sup>23</sup> Therefore, very long LCW lengths can be used without large energy losses.

Capillary tubing made from Teflon AF polymer has been applied previously as LCW. For example, the Teflon AF 2400 LCW has been used to enhance sensitivity in UV-visible spectroscopic measurements. As stated above, long lengths of LCW can be used that result in a long optical pathway through the liquid (to more than 25 m!) without large energy losses (see above): the signal is improved and the noise remains the same.<sup>25,26</sup> Teflon AF capillaries have also been applied in HPLC<sup>27</sup> and in gas analysis systems. Since the Teflon AF

polymer is very porous its physical properties allow for trapping of gases which in turn can be derivatized and products analyzed using, *e.g.*, UV-visible spectroscopy.<sup>28</sup> Furthermore, the Teflon AF LCW has also been applied in Raman and fluorescence spectroscopies.<sup>29,30</sup>

The experimental technique described below has been inspired from investigations using waveguide technology described above. To our best knowledge, this is the first work to apply the liquid core waveguide as a type of photolysis reactor to study kinetic reactions of atmospheric interest.

Again, the centrepiece of the experimental set-up is a liquid core waveguide made of Teflon AF 2400 (from BioGeneral, San Diego, CA). The Teflon AF 2400 guide had an inner and outer diameter of 200  $\mu\text{m}$  and 800  $\mu\text{m}$ , respectively. The length of the LCW was varied in the course of the study from 30 to 90 cm. In all cases, the internal volume of the liquid core waveguide was less than 0.1 mL for a maximum optical path length of 90 cm. Using very small liquid volumes in the LCW is one of the major advantages of using waveguides compared to a standard White cell design for studying radical liquid phase reactions. A good White cell can achieve a maximum path length of a few meters (which often requires expensive lasers) in a volume of *ca.* 50–100 mL. Such a large reaction volume requires much larger flow rates to replenish the cell between laser flashes. Under typical experimental conditions employed, the LCW can achieve much longer optical path lengths in much smaller volumes without requiring powerful light sources as those required in standard White cell systems for liquids. The application of the liquid core waveguide technology for laser flash photolysis studies will be presented elsewhere.

### Experimental approach

The Teflon waveguide photolysis system used for the reaction of OH with methanol, ethanol, tetrahydrofuran, dimethylmalonate, dimethylsuccinate, dimethylcarbonate and diethylcarbonate is shown schematically in Fig. 1. The highly flexible Teflon AF 2400 tubing was loosely coiled (*ca.* 4 cm diameter) around a 3 cm od Pyrex tube. The radiation from a medium pressure mercury UV lamp (Hereaus Noblelight, TQ150, 150 W) located within the Pyrex tube served as the photolytic light source. The cell was maintained at a constant temperature ( $\pm 0.5$  K) by circulating water that was allowed to flow from a thermostatically controlled cryostat bath (Huber cc230). The temperature of the system (*i.e.*, the Teflon coil and its contents) was constantly monitored using a Pt100 sensor. The Pt100 sensor/probe was placed in close contact with the waveguide coil. It was assumed that the reaction cell temperature was the same as the LCW and that no temperature gradient existed. Further, experiments were carried out to make sure that the mercury lamp did not heat the coil and

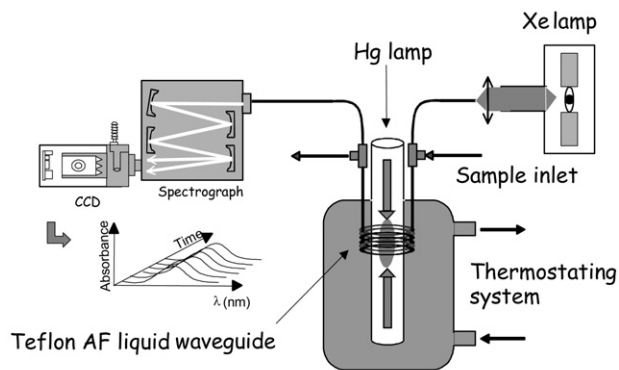


Fig. 1 Schematics of the LCW micro-flowtube experimental setup.

its contents. We did not observe any heating due to the mercury lamp since no increase in temperature was observed when the lamp was switched on. However, the Pt100 sensor used in this work had a stated uncertainty of  $\pm 0.15^\circ\text{C}$ . Given the uncertainty of the Pt100 sensor used in this work, we conservatively estimate that the uncertainty in the temperature in the Teflon coil and its contents resulting from heating by the lamp was  $\pm 0.30^\circ\text{C}$ . Therefore, we can safely state that the temperature rise caused by the UV lamp was less than  $0.30^\circ\text{C}$ .

A major fraction of the lamp output was filtered out by the water cooling liquid from the cryostat and the mercury lamp Pyrex housing. A fraction of the light ( $\lambda < 366\text{ nm}$ ) was transmitted through the LCW and its contents. The OH radicals were generated within the LCW following a mercury lamp photolysis of  $\text{H}_2\text{O}_2$  ( $\Phi = 1$  at  $\lambda \leq 366\text{ nm}$ ).<sup>31,32</sup> A quantum yield of  $\Phi = 1$  at  $\lambda \leq 366\text{ nm}$  was adopted to determine the initial OH radical concentration.<sup>31,32</sup> However, the effective quantum yield for the OH radical production in aqueous solutions may in fact be lower than 1. Thus, Zellner and coworkers and Zellner and Herrmann have reported  $\Phi^{\text{OH}} = 0.98$  and  $0.96$  at  $\lambda = 308$  and  $351\text{ nm}$ , respectively.<sup>33,34</sup> Values for  $\Phi^{\text{OH}}$  much less than 1 have been reported by Warneck, referring to the loss of  $\text{H}_2\text{O}_2$ .<sup>31,32</sup> However, the exact concentration of OH radicals is not very important for the outcome of this work, where nothing more is required than a major production of OH radicals.

The concentration of OH radicals in the aqueous phase was not directly measured but derived from the "titration" reaction resulting from a competition reaction of the OH radical with the  $\text{SCN}^-$  anion (see below). Under the experimental conditions employed, typical OH radical concentration was *ca.*  $10^{-8}\text{ mol L}^{-1}$ .

The geometry of the experimental setup (see Fig. 1) was such that it allowed for the reactant solution and the xenon lamp light to enter perpendicular to one another through a T-connector and the photolysing mercury lamp to be orthogonal to the waveguide reactor coil.

The solution content of the LCW was analyzed using UV-visible absorption spectroscopy (Andor Technology Fast Kinetics CCD) located in series to the direction of the propagation of both the solution and the xenon lamp light. The liquids were continuously pumped into the LCW through one entry of the T-connector, using a peristaltic pump (Watson-Marlow, type 323). Typical flow rates were in the range from  $0.1$  to  $3.0\text{ ml min}^{-1}$ . That is, the LCW was used as a micro-flowtube. In all cases, the time needed for the liquid to pass through the LCW was less than  $2\text{ s}$ . As a result, quite small irradiation times were achieved without expensive and technically involving experimental requirements. Under these experimental parameters, steady-state conditions were obtained within the LCW and verified experimentally (see below) but also theoretically using numerical simulations of the chemistry within the LCW. Theoretical calculations were performed using a Gear type solver (FACSIMILE<sup>35</sup>). All known rate and photolysis coefficients were directly taken from the solution kinetics database.<sup>3</sup>

In order to probe the solution contents of the LCW tube, the output of a  $75\text{ W}$  xenon lamp was focused on the entry of a  $100\text{ }\mu\text{m}$  diameter fused silica optical fibre. The fused silica optical fibre was held in the liquid content of the LCW tube. Then, the light was allowed to escape the solid optical fibre and collected in the liquid core waveguide. Again, the liquid core waveguide conducted the light up to its end where another fused silica optical fibre (located in the liquid) collected most of this transmitted light. This second solid optical fibre then conducted the light to the entry of a spectrograph (Lot-Oriel, 127i) coupled to a CCD camera (Andor Technology). The CCD allowed to monitor the evolution of the UV-visible spectrum as a function of wavelength and time within the LCW.

The  $(\text{SCN})_2^-$  anion spectra were recorded in the wavelength range from  $300$  to  $800\text{ nm}$ .

Given the experimental setup described above, the absorption spectra were integrated over the entire length of the LCW (*i.e.*, over time). However, FACSIMILE computer simulations showed that the steady state conditions were reached within a few milliseconds (*i.e.*, a few millimetres) of the LCW. This was below the observed experimental sensitivity limit and found not to affect the kinetic determinations of the rate coefficients and, therefore, ignored. We, therefore, believe that the integrated spectra can be safely attributed to the steady-state conditions achieved within the micro-flowtube.

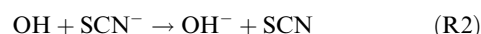
The observed  $(\text{SCN})_2^-$  anion spectra were corrected for the mercury lamp atomic lines trapped within the LCW during the photolysis of  $\text{H}_2\text{O}_2$ .

### Competition kinetics

Since the hydroxyl radical absorbs weakly in the visible region of the spectrum, it cannot be readily measured (at least when other absorbing compounds are present). Therefore, the OH radical concentration (or its temporal profile) has to be probed indirectly. This is commonly achieved using competition reaction kinetics.

Indeed, the OH radical can react either with a reactant RH (a generic organic compound for which the OH kinetics is unknown) or with the competitor (where the reaction coefficient is well established) where the reaction produces a transient species which absorbs strongly in the wavelength region of interest. Accordingly, the concentration of the transient species is then directly related to the number of OH radicals reacting with the competitor species. If the first reaction is fast, then the concentration of the absorbing species is low. Conversely, if the first reaction is slow then OH will have time to react with the competitor resulting in a high concentration of the absorbing species.

Among several potential competitors (for examples, see Table 1), the thiocyanate anion has been chosen because the product of its reaction with the OH radical [*i.e.*, the  $(\text{SCN})_2^-$  anion] exhibits the strongest extinction coefficient ( $\epsilon_{475\text{ nm}} = 7600\text{ M}^{-1}\text{ cm}^{-1}$ ).<sup>1</sup> The particular competition reaction system applied in this work is given below (R1–R5).



The reaction mechanism (R1)–(R4) has been studied by Chin and Wine.<sup>1</sup> These investigators report that the thiocyanate ion is a reliable competitor species that may be used to study OH radical reactions in the liquid phase.<sup>1</sup>

It must be underlined that this reaction mechanism is already simplified based on the work of Chin and Wine.<sup>1</sup> In fact, reaction (R2) proceeds in several steps but the corresponding details are not necessary for the competition approach used in this work and are, therefore, ignored. In fact, these authors showed that the OH radical is quantitatively converted into  $(\text{SCN})_2^-$  which may then be used as an OH radical concentration indicator. In fact, reaction (R3) is an equilibrium reaction and hence the  $(\text{SCN})_2^-$  anion is effectively the product of reaction (R2). As a result, for a given experiment, the  $(\text{SCN})_2^-$  anion concentration is proportional to the hydroxyl radical concentration.

In our study we adopted the temperature dependent rate coefficient for reaction (R2) reported by Chin and Wine ( $k_{\text{R2}} = 1.29 \times 10^{10}\text{ M}^{-1}\text{ s}^{-1}$  at  $298\text{ K}$ ).<sup>1</sup> Also, the inherent sensitivity of waveguides allowed us to work with low

**Table 1** Comparison of the room temperature rate coefficients for the reaction of the OH radical with methanol obtained in this work with literature values<sup>a</sup>

Technique	Competitor	$k_5/\text{M}^{-1} \text{s}^{-1}$	Ref.
PR	$\text{CO}_2^{2-}$	$8.8 \times 10^8$	36
PR	$\text{SCN}^-$	$7.8 \times 10^8$	36
PR	$\text{SCN}^-$	$1.0 \times 10^9$	37
PR	$\text{C}_6\text{H}_5\text{COO}^-$	$1.0 \times 10^9$	38
PR	$(\text{CH}_3)_2\text{NC}_6\text{H}_4\text{NO}$	$9.5 \times 10^8$	39
PR	Nitrobenzoate ion	$8.3 \times 10^8$	38
PR	$\text{C}_6\text{H}_5\text{CH}_2\text{COO}^-$	$8.3 \times 10^8$	38
PR	$[\text{Fe}(\text{CN})_6]^{4-}$	$9.7 \times 10^8$	40
PR	$\text{ABTS}^{2-b}$	$1.0 \times 10^9$	41
Literature review	Recommended value	$9.7 \times 10^8$	42
PR	$\text{SCN}^-$	$1.2 \times 10^9$	43
GR	$\text{C}_6\text{H}_5\text{COO}^-$	$8.3 \times 10^8$	44
MFT	$\text{SCN}^-$	$1.3 \times 10^9$	This work

<sup>a</sup> PR: pulse radiolysis; GR: gamma radiolysis; LP: laser photolysis; MFT: micro-flowtube. <sup>b</sup>  $\text{ABTS}^{2-}$ : 2,2'-azino-bis-(3-ethylbenzthiazole-6-sulfonate).

concentration of  $(\text{SCN}_2)^-$  anions. Under typical experimental conditions employed, the  $(\text{SCN}_2)^-$  anion concentration was *ca.*  $10^{-8} \text{ mol L}^{-1}$ . As a result, the  $(\text{SCN}_2)^-$  anions decayed by a first order process [see reaction (R4)].<sup>1</sup> At higher concentrations of  $(\text{SCN}_2)^-$  anions, the  $(\text{SCN}_2)^-$  anion decay may be governed by second order processes. However, the second order process for the decay of the  $(\text{SCN})_2^-$  anions was never observed under the experimental conditions employed in this work. In fact, Chin and Wine reported that the rate coefficient for reaction (R4) is  $870 \text{ s}^{-1}$ ,<sup>1</sup> while for the second order decay the rate coefficient was reported by these authors to be  $1.2 \times 10^9 \text{ L mol}^{-1} \text{ s}^{-1}$  at 298 K.<sup>1</sup> Since the  $(\text{SCN})_2^-$  anion concentrations were typically *ca.*  $10^{-8} \text{ mol L}^{-1}$ , the recombination of  $(\text{SCN})_2^-$  was not expected to be an important pathway for its removal. In the reaction mechanism (R1)–(R5), the  $(\text{SCN}_2)^-$  ion removal is believed to be governed by reaction (R4). This was confirmed experimentally in this work and is discussed in the result section of this paper.

The  $\text{SCN}^-$  anion was detected using UV-visible spectroscopy following a medium pressure mercury lamp photolysis of  $\text{H}_2\text{O}/\text{H}_2\text{O}_2/\text{reactant}/\text{KSCN}$  mixtures. All experiments for the reaction of the OH radical with oxygenates were carried out at room temperature (*i.e.*,  $T = 295\text{K}$ ). Assuming steady-state conditions for our flow conditions, the following expressions were derived from the reaction mechanism (R1)–(R5) (all processes are assumed to be first order or pseudo-first order under the experimental conditions employed).

$$2k_1[\text{H}_2\text{O}_2] - k_2[\text{OH}][\text{SCN}^-] - k_5[\text{OH}][\text{RH}] = 0 \quad (1)$$

$$k_2[\text{OH}][\text{SCN}^-] + k_{-3}[(\text{SCN}_2)^-] - k_3[\text{SCN}][\text{SCN}^-] = 0 \quad (2)$$

$$k_3[\text{SCN}][\text{SCN}^-] - k_{-3}[(\text{SCN}_2)^-] - k_4[(\text{SCN}_2)^-] = 0 \quad (3)$$

Using simple algebra, eqns. (1)–(3) can be rearranged to give the following relationship (eqn. 4).

$$\frac{1}{\text{Abs}} = \frac{1}{\text{Abs}_0} \left( 1 + \frac{k_5[\text{RH}]}{k_2[\text{SCN}^-]} \right) \quad (4)$$

In eqn. (4), Abs is the absorbance of the  $(\text{SCN})_2^-$  anion at a known concentration of the organic compound RH and  $\text{Abs}_0$  is the maximum  $(\text{SCN})_2^-$  anion absorbance in the absence of the reactant RH. Therefore, given the absorbencies,  $k_2$  and the concentration of the reactant RH, the rate coefficient  $k_5$  can easily be determined.

All experiments were carried out under “slow flow” conditions with a liquid linear flow rate through the micro-flowtube reactor of about  $1 \text{ m s}^{-1}$ . With this range of linear flow rates, the contents of the LCW were exposed to UV light only for short times (less than 2 s) ensuring that all reactant concentrations stayed constant, *i.e.*, secondary chemistry and degradation of  $\text{H}_2\text{O}_2$  or  $\text{SCN}^-$  was negligible and, therefore, ignored.

All error ranges, reported below, correspond to  $2\sigma$  uncertainties as simply derived from a linear fitting procedure of eqn. (4) to our data. As no specific statistical treatment was applied to our data (as Student's *t* factor considerations), these uncertainties are lower limits to the real uncertainty of our measurements.

## Reagents

Under the experimental conditions employed, typical hydrogen peroxide and thiocyanate concentrations (in units of  $\text{mol L}^{-1}$ ) were  $10^{-3}$  and  $2 \times 10^{-4}$ , respectively. Concentrations of the organic reagents used ranged from  $10^{-4}$  to  $10^{-2} \text{ mol L}^{-1}$  depending on the corresponding reactivities. The reagents used in this study had the following stated minimum purities: KSCN (Aldrich, >99%);  $\text{H}_2\text{O}_2$  (Aldrich, >30%), methanol (Merck, >99.9%) ethanol (Prolabo, >99.85%), tetrahydrofuran (Aldrich, >99.9%), dimethylmalonate (Aldrich, >99%), dimethylsuccinate (Aldrich, >98%), dimethylcarbonate (Fluka, >99%) and diethylcarbonate (Fluka, >99.5%) and were used without any further purification. All solutions were freshly prepared with non-degassed deionised water with resistivity >18 M $\Omega$ . Deionised water was prepared by passing tap water through a reverse osmosis demineralization filter (ATS Groupe Osmose) followed by a commercial deionizer (Millipore, Milli-Q). Dissolved oxygen within the water solution was shown not to be a problem and have any effect on the results presented in this work. Experiments were carried out in “regular” and degassed water. No difference in kinetics was observed.

## Results and discussion

### Validation of the technique

In order to check the consistency of the results obtained by this new technique, several well established rate constants have been remeasured.

### OH + methanol

The kinetics of the reaction of OH with methanol (R6) have been studied before (see for example Table 1).



However, the agreement among the reported values for the rate coefficient for the reaction of OH with methanol is less clear than the reported values for the reaction of OH with ethanol (see below). As a result, further investigations are warranted to better define the rate coefficient for the removal of OH by methanol.

Typical data for the absorption profiles of the  $(\text{SCN})_2^-$  concentration is shown in Fig. 2. The absorption profiles of the  $(\text{SCN})_2^-$  anion shown in Fig. 2 illustrate that the steady-state conditions are effectively reached within the LCW. The methanol concentration was varied from 0 to  $2 \times 10^{-3} \text{ mol L}^{-1}$ . In the data shown in Fig. 2, under typical experimental conditions employed the mercury lamp was triggered off for the first 20–30 s in order to flush the LCW with the solution of interest. Then the mercury lamp was triggered back on again and the  $(\text{SCN})_2^-$  ion monitored for about 150 s before triggering the lamp off again. The rise time of the  $(\text{SCN})_2^-$  ion signal (see

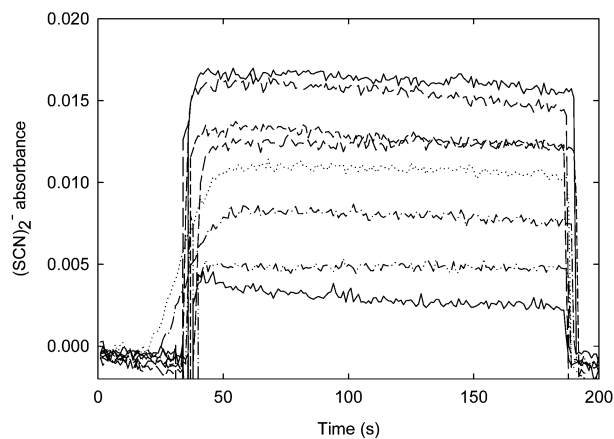


**Fig. 2** Typical  $(\text{SCN})_2^-$  anion concentration temporal profiles for 6 different methanol concentrations (from the top to the bottom line the methanol concentrations were  $0$ ,  $5 \times 10^{-5}$ ,  $2 \times 10^{-4}$ ,  $5 \times 10^{-4}$ ,  $1 \times 10^{-3}$  and  $2 \times 10^{-3}$  mol  $\text{L}^{-1}$ ). The UV lamp is switched on and off at ca. 30 and 180 s, respectively. The absorbance for the  $(\text{SCN})_2^-$  anion was taken in the 'plateau' region in the temporal range 150–180 s.

Fig. 2) was observed to depend on the mercury lamp temperature. Since the mercury lamp was triggered at different times for different durations depending on the experiment we did not control the starting temperature of the lamp. As a result, the  $(\text{SCN})_2^-$  ion signal rise times differed slightly from one trace to another. This did not pose a problem since all experimental conditions were reproducible leading to comparable absorbance profiles (see Fig. 2). Fig. 2 shows that the  $(\text{SCN})_2^-$  anion concentration, after the initial rise, decreases slightly with time, with an approximately 5% decrease in absorbance from 50 to 180 s. This seems to be more problematic when lower reactant concentrations (top two traces in Fig. 2) are used. However, this 'sloping' effect was weaker in the temporal range 150–180 s. As a result, the  $(\text{SCN})_2^-$  anion absorbance used in eqn. (4) was taken in the temporal range 150–180 s shown in Fig. 2. As mentioned, this sloping effect was mainly introduced by the stability of our mercury lamp.

The inverse absorbance plot for the  $(\text{SCN})_2^-$  anion versus the organic species concentration is shown in Fig. 3. The fit is obtained from linear least squares analysis to eqn. (4) and gives the relative rate constant,  $k_5$ . The major assumption used in eqn. (4) is that the decay of the  $(\text{SCN})_2^-$  anion is first order

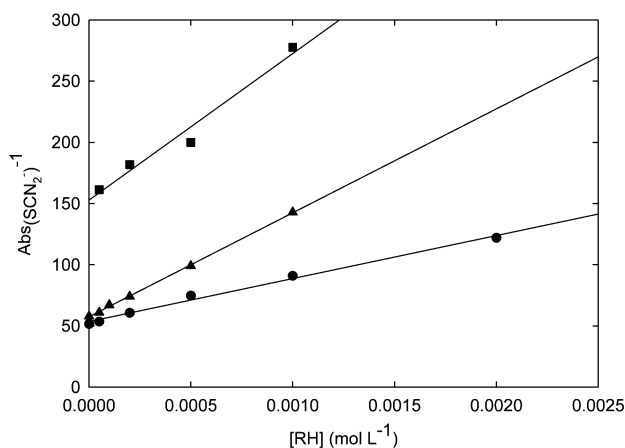


**Fig. 3** An inverse absorbance plot for  $(\text{SCN})_2^-$  as a function of the concentration of methanol (circle), ethanol (square) and THF (triangle). The fit is obtained from linear least squares analyses to eqn. (4). The slope of a linear fit to eqn. (4) yields the ratio of the rate coefficients for the OH + organic reactant and OH +  $\text{SCN}^-$  reactions.

and not a second order process. However, the data presented in Fig. 3 prove that the decay of the  $(\text{SCN})_2^-$  anion is a first order process and *not* a second order process. Since the decay of the  $(\text{SCN})_2^-$  anion shown in Fig. 3 is shown to be first order and *not* second order, reaction (R4) is believed to be the major reactive channel responsible for the removal of  $(\text{SCN})_2^-$  anions. As a result, eqn. (4) can be used to calculate the relative rate constant for the reaction of OH radical with organic species.

The rate coefficient for the reaction of OH with methanol at  $T = 295$  K obtained from a linear fit to eqn. (5) gives  $k_{\text{OH}+\text{methanol}} = (1.3 \pm 0.4) \times 10^9 \text{ M}^{-1} \text{ s}^{-1}$ . The uncertainty is  $\pm 2\sigma$  and represents precision only. Again, all uncertainties have been calculated based on uncertainties in temperature and absorption measurements.

The reported room temperature rate coefficient for the reaction of OH with methanol falls within the upper limit of the previously reported room temperature data (ranging from  $0.78$  to  $1.2 \times 10^9 \text{ M}^{-1} \text{ s}^{-1}$ ). However, certain room temperature studies failed to give specific experimental conditions or the specific experimental conditions were impossible to extract. At least part of the variations among previously reported data for the rate coefficient for the reaction of OH with methanol can be attributed to temperature effects. Many other relative rate measurements of the rate coefficient for the reaction of OH radical with methanol were carried out (see Table 1). In the majority of these studies the reported rate coefficients for the OH + methanol reaction is lower than that obtained in this study. However, all previous (with the exception of the work by Adams *et al.*<sup>43</sup>) investigations of the rate coefficient for the OH + methanol reaction were reported at higher pH values than the ones used in this work. One relative rate measurement of  $k_{\text{OH}+\text{methanol}}$  is reported in the literature that was carried out at pH values similar to the ones employed in this work. Thus, Adams *et al.*<sup>43</sup> have studied the reaction OH + methanol using a pulse radiolysis technique. These investigators obtained a value for  $k_{\text{OH}+\text{methanol}} = 1.2 \times 10^9 \text{ M}^{-1} \text{ s}^{-1}$ .<sup>43</sup> Similar to the experimental conditions employed in this work, Adams *et al.* obtained the rate coefficient for the reaction of the OH radical with methanol using the  $\text{SCN}^-$  ion as the competitor species. Moreover, similar to this work, Adams *et al.* performed their studies in solutions at low pH in order to minimize any adverse effects from secondary chemistry.<sup>43</sup> As a result, the rate coefficient for the reaction of OH with methanol reported in this study should only be compared with the work of Adams and co-workers whose work was performed under similar experimental conditions. Therefore, we find that the rate coefficient for the reaction of OH with methanol reported in this work is in excellent agreement with the previously reported value of  $1.2 \times 10^9 \text{ M}^{-1} \text{ s}^{-1}$  by Adams *et al.*<sup>43</sup>

Two other relative rate measurement of  $k_{\text{OH}+\text{methanol}}$  are reported in the literature that were carried out at lower pH values but used the  $\text{SCN}^-$  ion in their competition kinetics mechanism. Thus, Adams *et al.* and Elliot and McCracken obtain values for  $k_{\text{OH}+\text{methanol}} = 7.8 \times 10^8 \text{ M}^{-1} \text{ s}^{-1}$ <sup>36</sup> and  $1.0 \times 10^8 \text{ M}^{-1} \text{ s}^{-1}$ ,<sup>37</sup> respectively. These investigators used a value of  $1.1 \times 10^{10} \text{ M}^{-1} \text{ s}^{-1}$  for the rate coefficient for the competition reaction of the OH radical with  $\text{SCN}^-$ . In this work we adopted a rate coefficient of  $1.29 \times 10^9 \text{ M}^{-1} \text{ s}^{-1}$  reported by Chin and Wine<sup>1</sup> for the OH +  $\text{SCN}^-$  reaction. This rate coefficient is 17% higher than the value used by Adams *et al.* and Elliot and McCracken. A correction of Adams's *et al.* and Elliot and McCracken's result upward by 17% gives  $k_{\text{OH}+\text{methanol}} = 0.91 \times 10^9$  and  $1.2 \times 10^9 \text{ M}^{-1} \text{ s}^{-1}$ , respectively, a range of values which agree well with the rate coefficient for the OH + methanol reaction obtained in this work.

Based on the results obtained in this work for the reaction of OH with methanol we can report with confidence that the new experimental approach used in this study gives results that are

**Table 2** Comparison of the room temperature rate coefficients for the reaction of the OH radical with ethanol obtained in this work with literature values<sup>a</sup>

Technique competitor	Competitor	$k_5/\text{M}^{-1} \text{s}^{-1}$	Ref.
GR	$\text{C}_6\text{H}_5\text{COO}^-$	$1.7 \times 10^9$	45
PR	$\text{SCN}^-$	$1.8 \times 10^9$	36
PR	$\text{CO}_3^{2-}$	$1.9 \times 10^9$	43
PR	$[\text{Fe}(\text{CN})_6]^{4-}$	$2.2 \times 10^9$	46
PR	$\text{HSO}_4^-$	$2.0 \times 10^9$	47
PR	$(\text{CH}_3)_2\text{NC}_6\text{H}_4\text{NO}$	$1.6 \times 10^9$	39
PR	$\text{C}_6\text{H}_5\text{CH}_2\text{COO}^-$	$1.8 \times 10^9$	38
PR	Nitro benzoate ion	$1.8 \times 10^9$	38
PR	$\text{C}_6\text{H}_5\text{COO}^-$	$1.8 \times 10^9$	38
PR	$\text{CO}_3^{2-}$	$2.1 \times 10^9$	48
PR	$[\text{Fe}(\text{CN})_6]^{4-}$	$2.1 \times 10^9$	40
PR	$[\text{Fe}(\text{CN})_6]^{4-}$	$1.9 \times 10^9$	49
PR	$\text{ABTS}^{2-b}$	$1.9 \times 10^9$	41
Literature review	Recommended value	$1.9 \times 10^9$	42
PR	$[\text{Fe}(\text{CN})_6]^{4-}$	$1.9 \times 10^9$	50
GR	$\text{C}_6\text{H}_5\text{COO}^-$	$2.2 \times 10^9$	44
LP	$\text{SCN}^-$	$2.1 \times 10^9$	51
MFT	$\text{SCN}^-$	$1.9 \times 10^9$	This work

<sup>a</sup> PR: Pulse radiolysis; GR: Gamma radiolysis; LP: Laser photolysis; MFT: Micro-flowtube. <sup>b</sup>  $\text{ABTS}^{2-}$ : 2,2'-azinobis-(3-ethylbenzthiazoline-6-sulfonate).

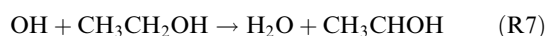
in good agreement with the previously reported data using other well established and proven techniques.

### OH + ethanol

Many room temperature studies of the OH + ethanol reaction kinetics are reported in the literature (see Table 2).

Absorbance data of the  $(\text{SCN})_2^-$  ion concentration at different concentrations of ethanol obtained in this work, are similar to the one shown in Fig. 2 for methanol. The absorbance profile of the  $(\text{SCN})_2^-$  anion was observed to decrease with increasing ethanol concentration. This is in agreement with the fundamentals of the competition kinetics.

An inverse absorbance plot for  $(\text{SCN})_2^-$  at  $\lambda = 480 \text{ nm}$  as a function of ethanol concentration is shown in Fig. 3. The fit is obtained from linear least squares analyses to eqn. (4). The slope of a linear fit to eqn. (4) yields the ratio of the rate coefficients for the OH + ethanol and OH +  $\text{SCN}^-$  reactions. Since the rate coefficient for the OH +  $\text{SCN}^-$  reaction is known, the rate coefficient for the reaction of OH with ethanol [*i.e.*, reaction (R7)] can easily be determined using simple algebra.



The rate coefficient for the aqueous phase reaction of the OH radical with ethanol at  $T = 295 \text{ K}$  obtained in this work is  $k_{\text{OH}+\text{ethanol}} = (1.9 \pm 0.5) \times 10^9 \text{ M}^{-1} \text{ s}^{-1}$ . The uncertainty is  $\pm 2\sigma$  and represents precision only. The rate coefficient for the OH + ethanol reaction reported in this study compares very well with the available literature data (see Table 2) independent of the competitor species used.

### OH + tetrahydrofuran

Absorbance data of the  $(\text{SCN})_2^-$  ion concentration at different concentrations of THF obtained in this work are similar to the one shown in Fig. 2 for methanol. An inverse absorbance plot of the inverse for  $(\text{SCN})_2^-$  at  $\lambda = 480 \text{ nm}$  as a function of THF concentration ranging from 0 to  $1 \times 10^{-3} \text{ mol L}^{-1}$  is shown in Fig. 3. Similar to the situation described above, the fit is

obtained from linear least squares analyses to eqn. (4). The observed rate coefficient for the removal of OH by THF at  $T = 298 \text{ K}$  is found to be  $(3.8 \pm 1.0) \times 10^9 \text{ M}^{-1} \text{ s}^{-1}$ . The uncertainty is  $\pm 2\sigma$  and represents precision only.

The reaction of OH with tetrahydrofuran (R8) was the focus of only one previous investigation carried out by Eibenberger.<sup>52</sup> This investigator reported a rate coefficient for (R8) to be  $3.8 \times 10^9 \text{ M}^{-1} \text{ s}^{-1}$  at  $T = 298 \text{ K}$ .

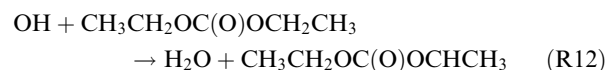
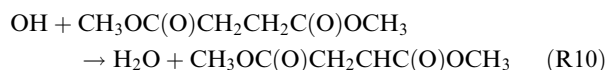
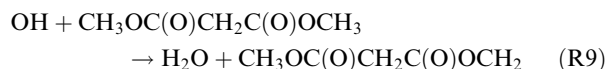


The value for the OH + THF reaction rate coefficient reported in this work is in excellent agreement with the data obtained by Eibenberger.<sup>52</sup>

Since the reported rate coefficients for the reactions of OH with ethanol, methanol and THF agree very well with the literature data, we report with confidence that the new experimental approach used in this study is scientifically sound and reliable to be applied to carry out the following and any relative future liquid phase kinetic experiments.

### Determination of new rate constants

In the atmosphere, the degradation of the dimethylmalonate, dimethylsuccinate, dimethylcarbonate and diethylcarbonate will most likely be influenced by the OH radical attack [*i.e.*, reactions (R9)–(R12)].



The experimental approach described above was used to measure the bimolecular rate coefficients for the reactions of the OH radical with dimethylmalonate (R9), dimethylsuccinate (R10), dimethylcarbonate (R11) and diethylcarbonate (R12).

Again, absorbance data of the  $(\text{SCN})_2^-$  ion concentration at different concentrations of dimethylmalonate, dimethylsuccinate, dimethylcarbonate and diethylcarbonate obtained in this work are similar to the one shown in Fig. 2 for methanol.

Inverse absorbance plots for  $(\text{SCN})_2^-$  at  $\lambda = 480 \text{ nm}$  at different concentrations of dimethylmalonate, dimethylsuccinate, dimethylcarbonate and diethylcarbonate are shown in Fig. 4.

The obtained rate coefficients for the reactions of the OH radical with dimethylmalonate, dimethylsuccinate, dimethylcarbonate and diethylcarbonate carried out at  $T = 295 \text{ K}$  are summarized in Table 3. To our best knowledge, there are no other kinetic data for reactions (R9)–(R12) reported in the literature with which to compare our results. However, bond energies for the reactions of the OH radical with the 7 oxygenates shown in Table 4, tend to support the idea that the reactivity of the oxygenates toward the attack by the OH radical is linked to the steric environment of the  $-\text{C}(\text{O})\text{O}-$  functional group. This important point is discussed in the following section.

### Discussion

A major assumption in the reactions studied above is that the OH attack on the alcohol, ester or carbonate proceeds *via* a H-abstraction mechanism. This is consistent with the large volume chamber study of the reaction of the OH radical with DBE-5 in the presence of NO carried out by Atkinson and

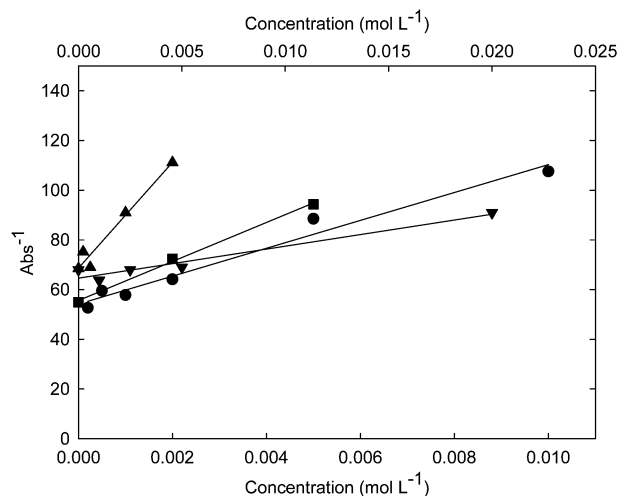


**Fig. 4** An inverse absorbance plot for the oxygenates as a function of their concentration [according to eqn. (1)]. The slope of the fitted line is a measure of the ratio of the reference to oxygenate rate constants. (Bottom axis: ● dimethylmalonate, ■ dimethylsuccinate, and ▲ diethylcarbonate; top axis: ▼ dimethylcarbonate).

co-workers. These investigators report that the OH radical reaction with DBE-5 proceeds by three pathways, all involving H-atom abstraction from the C–H bonds.<sup>11</sup> If the OH attack proceeds *via* a H-abstraction, then the observed rate coefficient constants should be correlated with the type of bond and bond strength of the “leaving” hydrogen atom. The “leaving” hydrogen atom is probably the one having the weakest C–H bond strength (it was assumed that no H-abstraction occurs at the O–H group for alcohols). Bond dissociation energies (BDE) of the weakest C–H for methanol, ethanol, tetrahydrofuran, dimethylmalonate, dimethylsuccinate, dimethylcarbonate and diethylcarbonate are listed in Table 4. Other parameters listed in Table 4 are: (i) the number of equivalent hydrogen atom  $n_{\text{H}}$  (*i.e.*, those having the weakest bond strength) and (ii) logarithm of the rate per H atom  $k_{\text{H}}$  which is derived by:

$$k_{\text{H}} = k_{\text{obs}}/n_{\text{H}} \quad (5)$$

Many of the bond dissociation energies have not been experimentally measured and were, therefore, estimated using semi-empirical group contribution methods.<sup>53,54</sup> It might be assumed that the observed reactivity differences of the OH radical toward the organic species considered are due to changes in the activation energies which are expected to be linked to the bond dissociation energy of the bond being ruptured.<sup>55</sup> If this is the case, there should be a linear dependence of logarithm of  $k_{\text{H}}$  on the bond strength. A plot of  $\log(k_{\text{H}})$  versus BDE is shown in Fig. 5. As can be seen in Fig. 5, there is indeed a (weak) correlation between the logarithm of  $k_{\text{H}}$  and the bond strength, *i.e.*, a decrease of the rate coefficient is observed with increasing BDE. As a result, the reaction of

**Table 3** Summary of the rate coefficients for the reactions of the OH radical with four oxygenates obtained in this work

Organic species	$k^{abc}$
Dimethylcarbonate	$k_9 = (5.1 \pm 2.2) \times 10^7$
Diethylcarbonate	$k_{10} = (7.9 \pm 3.2) \times 10^8$
Dimethylmalonate	$k_{11} = (2.7 \pm 0.9) \times 10^8$
Dimethylsuccinate	$k_{12} = (5.3 \pm 2.9) \times 10^8$

<sup>a</sup> All experiments performed at  $T = 295$  K. <sup>b</sup> Units are  $k(\text{M}^{-1} \text{s}^{-1})$ . <sup>c</sup> Uncertainties are  $\pm 2\sigma$  and represent precision only.

**Table 4** Number of equivalent weak C–H bonds ( $n_{\text{H}}$ ) with the bond dissociation energy (BDE) and the logarithm of the rate constant per C–H bond caption

Species	$n_{\text{H}}$	BDE/ $\text{kJ mol}^{-1}$	$\text{Log}(k_{\text{H}})$
Methanol	3	385	8.637
Ethanol	2	393	8.978
THF	4	382	8.978
Dimethylmalonate	6	444	7.653
Dimethylsuccinate	4	424	8.122
Dimethylcarbonate	6	431	6.929
Diethylcarbonate	4	424	8.296

the OH radical with oxygenates proceeds *via* a H-atom abstraction mechanism. However, dimethyl carbonate does not seem to fit the pattern. The reason for this is not clear. As a consequence, the weakness of the correlation does not, currently, allow any reliable attempt of building an estimation method for the OH radical rate coefficients. While it seems unlikely that the reaction of the OH radical with oxygenates does not proceed *via* a H-atom abstraction mechanism, this issue remains to be conclusively resolved. Clearly, more theoretical and experimental research is needed to understand the H-atom abstraction mechanism of the OH + oxygenates reaction. Accordingly, any future research is warranted on the reactivity of free radicals in aqueous solutions.

## Conclusion

This work addressed the oxidation of several oxygenated compounds by the hydroxyl radical using a newly developed experimental technique. The experimental approach described herein takes advantage of the novel liquid core waveguide technology of Teflon AF 2400. The physical nature of waveguides allows for the construction of photolysis reaction cells with very low volumes but potentially very long optical path lengths. As a result, the Teflon waveguide photolysis system described here is potentially a very powerful and cost-effective technique to study liquid phase chemistry with potentially very low detection limits of chemical transients.

In summary, we have successfully applied optical waveguides to measure rate coefficients for the liquid phase reaction of the OH radical with methanol, ethanol, tetrahydrofuran, dimethylmalonate, dimethylsuccinate, dimethylcarbonate and diethylcarbonate. The reported rate coefficients for the reactions of OH with ethanol, methanol and THF agree very well

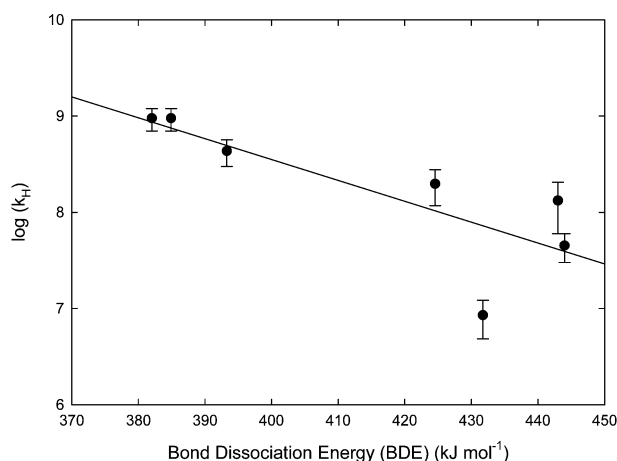


**Fig. 5** Plot of  $\log(k_{\text{H}})$  vs. bond dissociation energy. Uncertainties are  $\pm 2\sigma$  and represent precision only.

with the literature values. To date, there is no kinetic data reported for the OH radical reaction with dimethylmalonate, dimethylsuccinate, dimethylcarbonate and diethylcarbonate with which to compare our results.

## Acknowledgements

Support of this work by the Programme National de Chimie Atmosphérique (PNCA) from the CNRS is gratefully acknowledged and the project PRIMEQUAL by the French Minister for Environment. The authors also thank the anonymous reviewers for their critical and helpful comments and G. V. Buxton and G. A. Salmon for having provided the initial push into that field.

## References

- M. Chin and P. H. Wine, *J. Photochem. Photobiol., A*, 1992, **69**, 17–25.
- A. E. Huie, in *Laboratory Studies of Atmospheric Heterogeneous Chemistry; Current Problems in Atmospheric Chemistry, Advances in Physical Chemistry Series*, ed. J. R. Barker, World Scientific, Singapore, 1994, vol. 3, pp. 374–419.
- A. B. Ross, W. G. Mallard, W. P. Helman, G. V. Buxton, R. E. Huie and P. Neta, 1998, NDRL-NIST Solution Kinetics Database, National Institute of Standards and Technology (NIST), see also <http://www.rcdc.nd.edu>.
- M. Uusi-Penttilä, R. J. Richards, P. Blowers, B. A. Torgerson and K. A. Berglund, *J. Chem. Eng. Data*, 1996, **41**, 235–238.
- F. Cavalli, I. Barnes and K. H. Becker, *Int. J. Chem. Kinet.*, 2001, **33**, 431–439.
- J. Wenger, E. Porter, E. Collins, J. Treacy and H. Sidebottom, *Chemosphere*, 1999, **38**, 1197–1204.
- M. Bilde, T. E. Mögelberg, J. Sehested, O. J. Nielsen, T. J. Wallington, M. D. Hurley, S. M. Japar, M. Dill, V. L. Orkin, T. J. Buckley, R. E. Huie and M. J. Kurylo, *J. Phys. Chem. A*, 1997, **101**, 3514–3525.
- M. A. Pacheco and C. L. Marshall, *Energy Fuels*, 1997, **11**, 2–29.
- J. R. Odum, T. P. W. Jungkamp, R. J. Griffin, R. C. Flagan and J. H. Seinfeld, *Science*, 1997, **276**, 96–99.
- J. H. Seinfeld and S. N. Pandis, *Atmospheric Chemistry and Physics: From Air Pollution to Climate Change*, Wiley, New York, 1998.
- E. C. Tuazon, S. M. Aschmann and R. Atkinson, *Environ. Sci. Technol.*, 1999, **33**, 2885–2890.
- C. von Sonntag and H.-P. Schuchmann, *Angew. Chem. Int. Ed. Engl.*, 1991, **30**, 1229–1253.
- P. H. Wine, R. L. Mauldin and R. P. Thorn, *J. Phys. Chem.*, 1988, **92**, 1156–1162.
- G. V. Buxton, M. Bydder and G. A. Salmon, *J. Chem. Soc., Faraday Trans.*, 1998, **94**, 653–657.
- G. V. Buxton, T. N. Malone and G. A. Salmon, *J. Chem. Soc., Faraday Trans.*, 1997, **93**, 2889–2891.
- G. V. Buxton, T. N. Malone and G. A. Salmon, *J. Chem. Soc., Faraday Trans.*, 1996, **92**, 1287–1289.
- G. V. Buxton, S. McGowan, G. A. Salmon, J. E. Williams and N. D. Wood, *Atmos. Environ.*, 1996, **30**, 2483–2493.
- H. Herrmann, M. Exner, H. W. Jacobi, G. Raabe, A. Reese and R. Zellner, *Faraday Discuss.*, 1995, **100**, 129–153.
- H. Herrmann, H. W. Jacobi, G. Raabe, A. Reese and R. Zellner, *Fresenius J. Anal. Chem.*, 1996, **355**, 343–344.
- H. Herrmann, A. Reese, F. Wicktor and R. Zellner, *J. Mol. Struct.*, 1997, **408**, 539–542.
- H. Herrmann, A. Reese and R. Zellner, *J. Mol. Struct.*, 1995, **348**, 183–186.
- R. Altkorn, I. Koev and M. J. Pelletier, *Appl. Spectrosc.*, 1999, **53**, 1169–1176.
- R. Altkorn, I. Koev, R. P. Van Duyne and M. Litorja, *Appl. Opt.*, 1997, **36**, 8992–8998.
- W. Groh and A. Zimmermann, *Macromolecules*, 1991, **24**, 6660–6663.
- R. D. Waterbury, W. S. Yao, R. H. Byrne, B. J. Marquardt, K. P. Turney and L. W. Burgess, *Anal. Chim. Acta*, 1997, **357**, 99–102.
- C. Gooijer, G. P. Hoornweg, T. deBeer, A. Bader, D. J. van Iperen and U. A. T. Brinkman, *J. Chromatogr.*, 1998, **824**, 1–5.
- R. H. Byrne, W. S. Yao, E. Kaltenbacher and R. D. Waterbury, *Talanta*, 2000, **50**, 1307–1312.
- P. K. Dasgupta, S. Y. Liu and H. Fein, *Eur. Pat. Appl.*, 1999, 15.
- B. J. Marquardt, P. G. Vahey, R. E. Synovec and L. W. Burgess, *Anal. Chem.*, 1999, **71**, 4808–4814.
- J. Z. Li, P. K. Dasgupta and Z. Genfa, *Talanta*, 1999, **50**, 617–623.
- P. Warneck, *Heterogeneous and Liquid Phase Processes, Laboratory Studies Related to Aerosols and Clouds*, Springer, Berlin, 1996.
- B. J. Finlayson-Pitts and J. N. Pitts, *Chemistry of the Upper and Lower Atmosphere, Theory, Experiments, and Applications*, Academic Press, San Diego, 2000.
- R. Zellner, M. Exner and H. Herrmann, *J. Atmos. Chem.*, 1990, **10**, 411–425.
- R. Zellner and H. Herrmann, in *Spectroscopy in Environmental Science*, ed. R. J. H. Clark and R. E. Hester, John Wiley & Sons Ltd., 1995, pp. 381–451.
- AEA Technology, 1998, FACSIMILE for Windows, A Program for Modelling Kinetics and Transport Under Windows 95 and NT, <http://www.mcpa-software.com/facsimileframe.html>.
- G. E. Adams, J. W. Boag and B. D. Michael, *Trans. Faraday Soc.*, 1965, **61**, 1417–1424.
- A. J. Elliot and D. R. McCracken, *Radiat. Phys. Chem.*, 1989, **33**, 69–74.
- P. Neta and L. M. Dorfman, *J. Phys. Chem.*, 1969, **73**, 413–417.
- J. H. Baxendale and A. A. Khan, *Int. J. Radiat. Phys. Chem.*, 1969, **1**, 11–24.
- R. L. Willson, C. L. Greenstock, G. E. Adams, R. Wageman and L. M. Dorfman, *Int. J. Radiat. Phys. Chem.*, 1971, **3**, 211–220.
- B. S. Wolfenden and R. L. Willson, *J. Chem. Soc., Perkin Trans. 2*, 1982, 805–812.
- G. V. Buxton, C. L. Greenstock, W. P. Helman and A. B. Ross, *J. Phys. Chem. Ref. Data*, 1988, **17**, 513–886.
- G. E. Adams, J. W. Boag, J. Currant and B. D. Michael, in *Pulse Radiolysis*, ed. M. Ebert, J. P. Keene, A. J. Swallow and J. H. Baxendale, Academic Press, New York, 1965, pp. 131–143.
- N. Motohashi and Y. Saito, *Chem. Pharm. Bull.*, 1993, **41**, 1842–1845.
- R. W. Matthews and D. F. Sangster, *J. Phys. Chem.*, 1965, **69**, 1938–1946.
- G. E. Adams, J. W. Boag and B. D. Michael, *Trans. Faraday Soc.*, 1965, **61**, 492–505.
- E. Heckel, A. Henglein and G. Beck, *Ber. Bunsen-Ges. Physik. Chem.*, 1966, **70**, 149–154.
- G. V. Buxton, *Trans. Faraday Soc.*, 1970, **66**, 1656–1660.
- M. S. Matheson, A. Mamou, J. Silverman and J. Rabani, *J. Phys. Chem.*, 1973, **77**, 2420–2424.
- H. R. Park and N. Getoff, *Z. Naturforsch., A: Phys. Sci.*, 1992, **47**, 985–991.
- B. Ervens and H. Herrmann, *Phys. Chem. Chem. Phys.*, 2002, submitted.
- J. Eibenberger, PhD Thesis, *Pulse Radiolytic Investigations Concerning the Formation and Oxidation of Organic Radicals in Aqueous Solutions*, University of Vienna, 1980.
- J. Gasteiger, in *Physical Property Prediction in Organic Chemistry*, ed. C. Jochum, M. G. Hicks and J. Sunkel, Springer Verlag, Heidelberg, 1988, pp. 119–138.
- J. Gasteiger, 2000, PETRA Parameter Estimation for the Treatment of Reactivity Applications, <http://www2.chemie.uni-erlangen.de/software/petra/>.
- C. L. Clifton and R. E. Huie, *Int. J. Chem. Kinet.*, 1989, **21**, 677–687.